Supplementary Information for

"Engineering modular and tunable genetic amplifiers for scaling transcriptional signals in cascaded gene networks"

Baojun Wang[1,3], Mauricio Barahona[2] & Martin Buck[3]

[1]*Centre for Synthetic and Systems Biology, School of Biological Sciences, University of Edinburgh, Edinburgh, EH9 3JR, UK.*
[2]*Department of Mathematics, Faculty of Natural Sciences, Imperial College London, London, SW7 2AZ, UK.*
[3]*Department of Life Sciences, Faculty of Natural Sciences, Imperial College London, London, SW7 2AZ, UK.*

Table of Contents

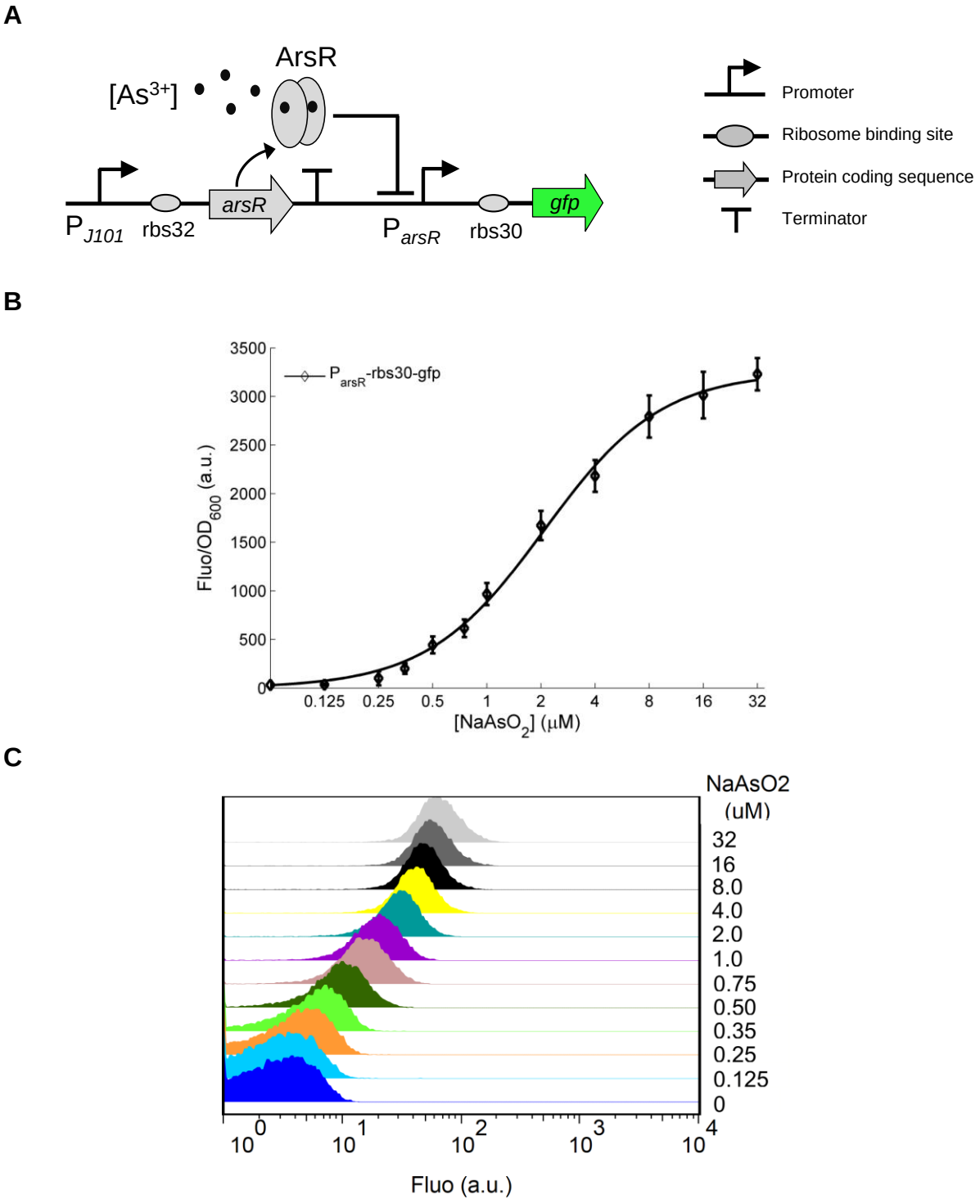

Figure S1: Design and characterization of the arsenic responsive sensor. (**A**) The architecture of the arsenic responsive sensor. The arsenic sensor is designed with the arsenite responsive ArsR expressed under control of a constitutive promoter J105 and with *gfp* fused to the ArsR repressed promoter P_{arsR} as the output reporter. (**B**) The fitted transfer function of the arsenic input sensor against experimental data (Table S1). (**C**) The single cell flow cytometry data shows the cellular responses of the arsenic sensor induced by varied arsenic concentrations (0, 0.125, 0.25, 0.35, 0.5, 0.75, 1.0, 2.0, 4.0, 8.0, 16, 32 μM $NaAsO_2$).

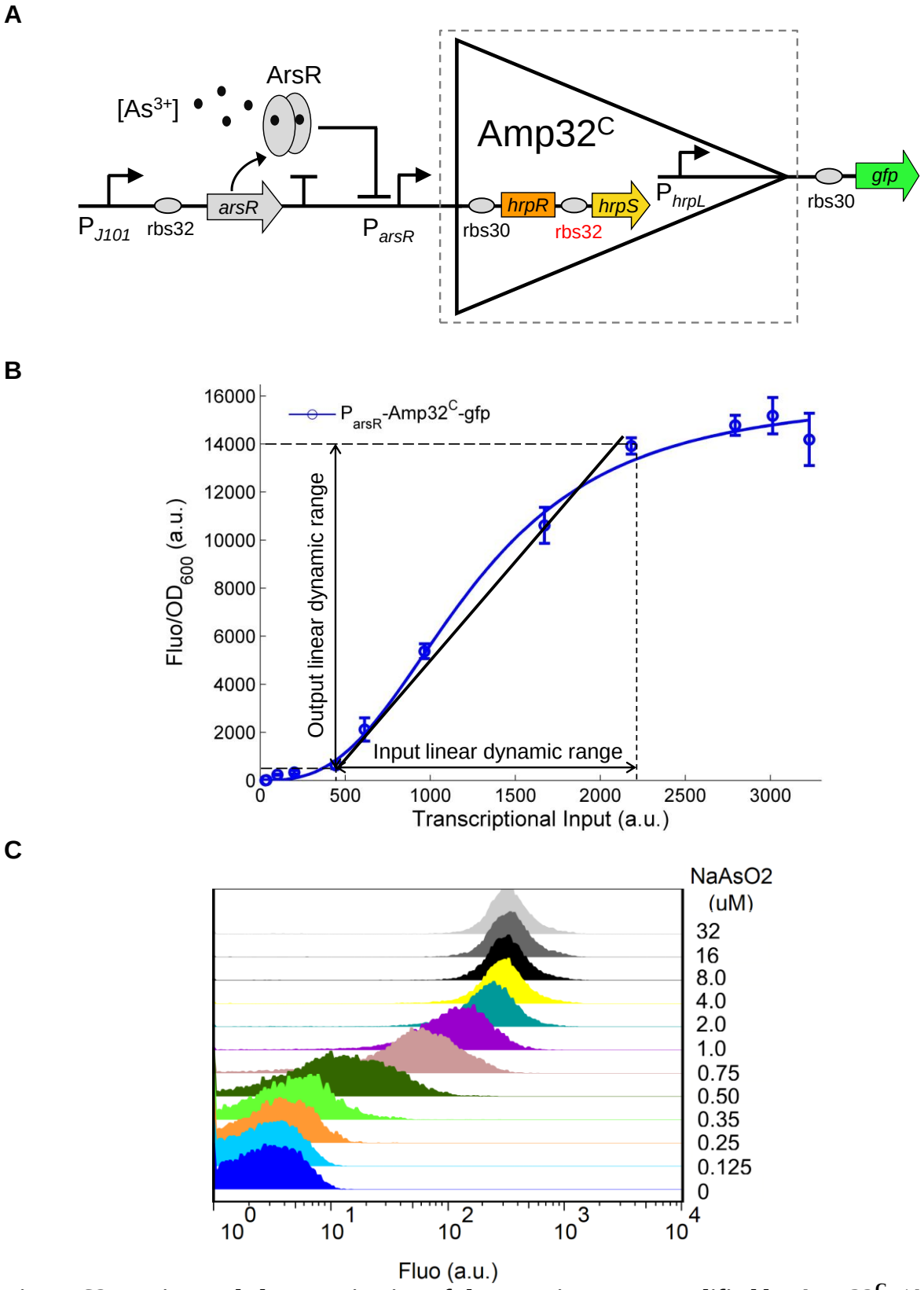

Figure S2: Design and characterization of the arsenic sensor amplified by Amp32^{C}. (**A**) The arsenic sensor input is coupled to Amp32^{C} before cascaded to the *gfp* output. (**B**) The fitted transfer function of Amp32^{C} against the experimental data (Table S2). The device operating range used for linear fitting is also shown. (**C**) The single cell flow cytometry data shows the cellular responses of the amplified arsenic sensor induced by varied arsenic concentrations (0, 0.125, 0.25, 0.35, 0.5, 0.75, 1.0, 2.0, 4.0, 8.0, 16, 32 μM $NaAsO_2$).

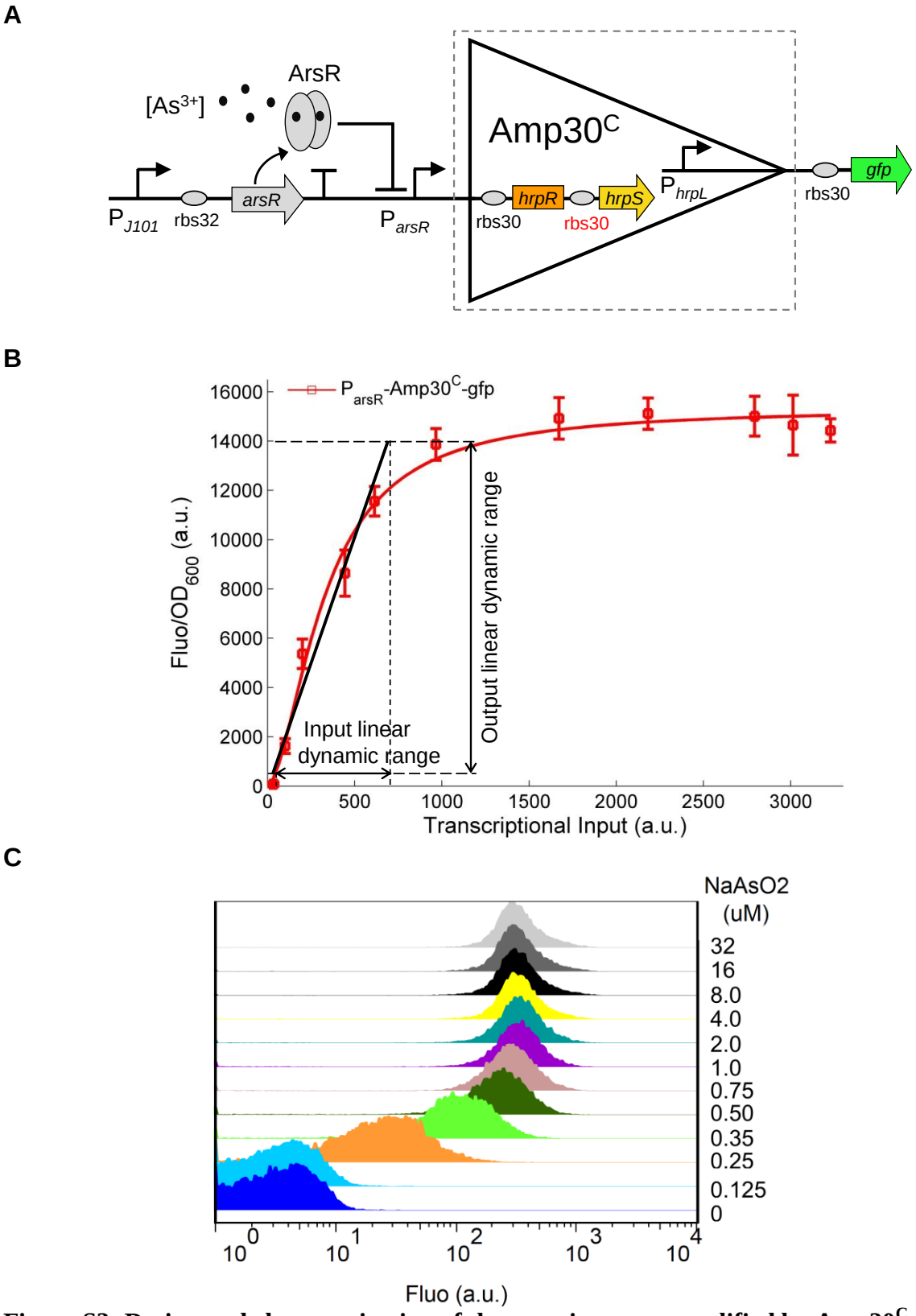

Figure S3: Design and characterization of the arsenic sensor amplified by Amp30^C. (**A**) The arsenic sensor input is coupled to Amp30^C before cascaded to the *gfp* output. (**B**) The fitted transfer function of Amp30^C against the experimental data (Table S2). The device operating range used for linear fitting is also shown. (**C**) The single cell flow cytometry data shows the cellular responses of the amplified arsenic sensor induced by varied arsenic concentrations (0, 0.125, 0.25, 0.35, 0.5, 0.75, 1.0, 2.0, 4.0, 8.0, 16, 32 μM $NaAsO_2$).

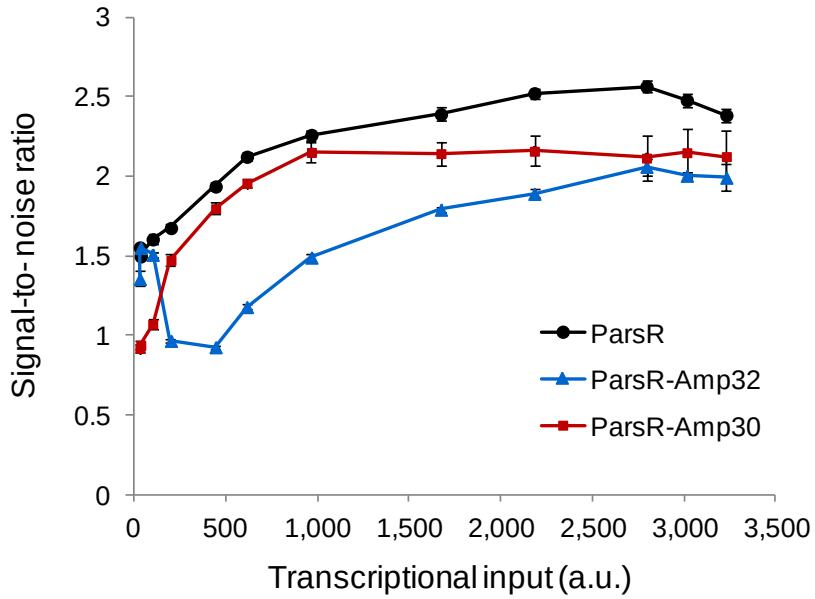

Figure S4: The signal-to-noise ratios of the arsenic input sensor without amplification and with amplification by Amp32^{C} and Amp30^{C}. The signal-to-noise ratio (SNR) is calculated as the ratio of the sample fluorescent mean to the standard deviation of the cell population from the single cell flow cytometry assay (Fig. S1C - S3C), i.e. SNR= μ/σ^{1}**.** Data are means and s.d. for three replicates.

A

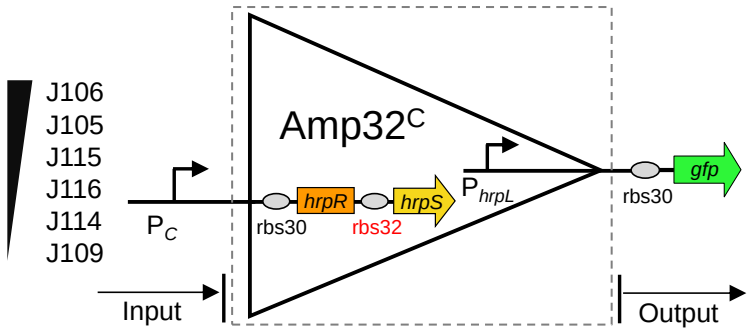

B

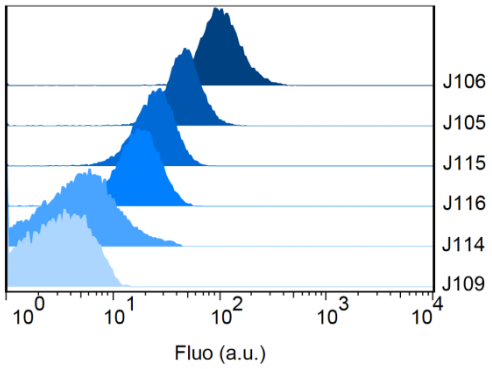

C

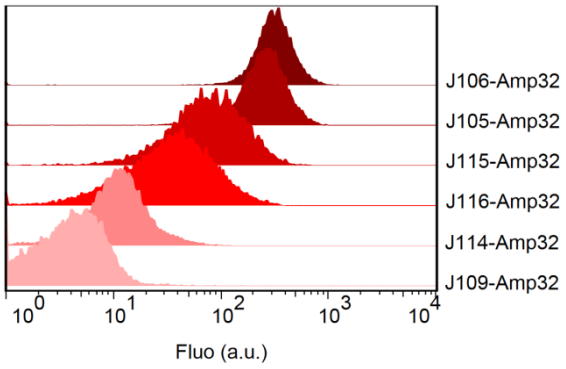

Figure S5: Single cell characterization of Amp32^{C} with constitutive promoter inputs. (**A**) Schematic showing the fixed gain amplifier Amp32^{C} with constitutive promoter as the signal input. The single cell flow cytometry data shows the cellular responses of the 6 constitutive promoters (**B**) and those amplified by Amp32^{C} (**C**). The results demonstrate a consistent enhancing effect of the amplifier across the whole cell population with modest cell to cell variability being evident.

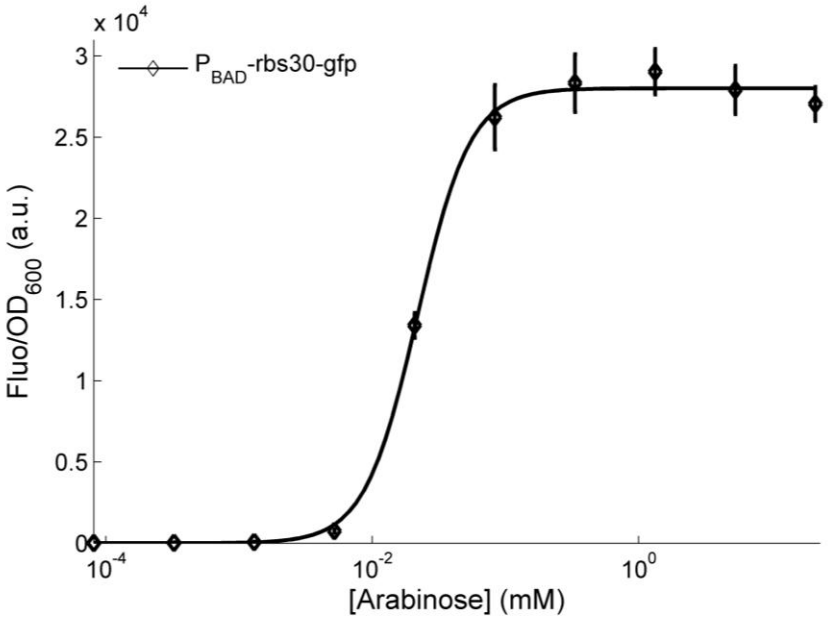

Figure S6: The transfer function of the characterised P_{BAD} promoter. The data were collected in *E. coli* TOP10 in LB media 5 hrs after induction by varied arabinose concentrations (0, 1.3 × 10^{-3}, 5.2 × 10^{-3}, 2.1 × 10^{-2}, 8.3 × 10^{-2}, 0.33, 1.33, 5.32 and 21.2 mM) and fitted to inducible promoter transfer function equation S2 (Table S1).

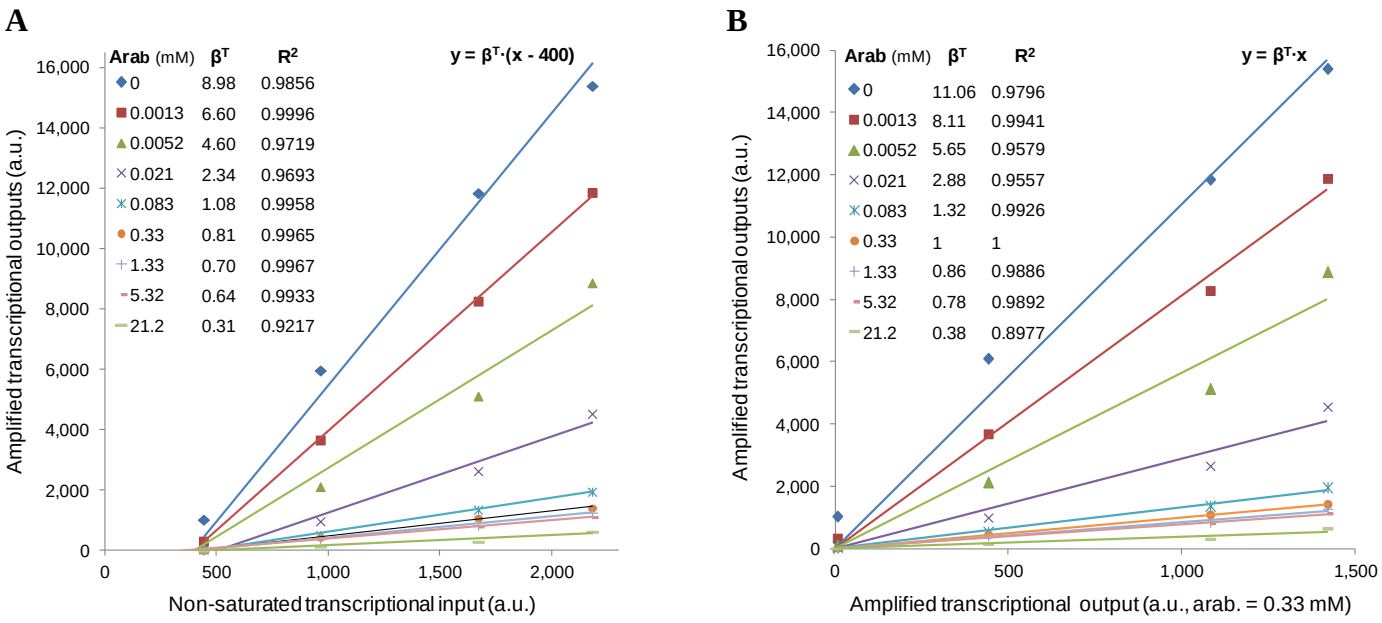

Figure S7: (A) Scatter plot showing the linearity between the non-saturated inputs and their amplified outputs of $Amp32^T$ under different gains as in Fig. 4B by fitting to a linear model. **(B)** Scatter plot showing the linearity between the amplified transcriptional outputs of $Amp32^T$ under different amplification gains as shown in Fig. 4B.

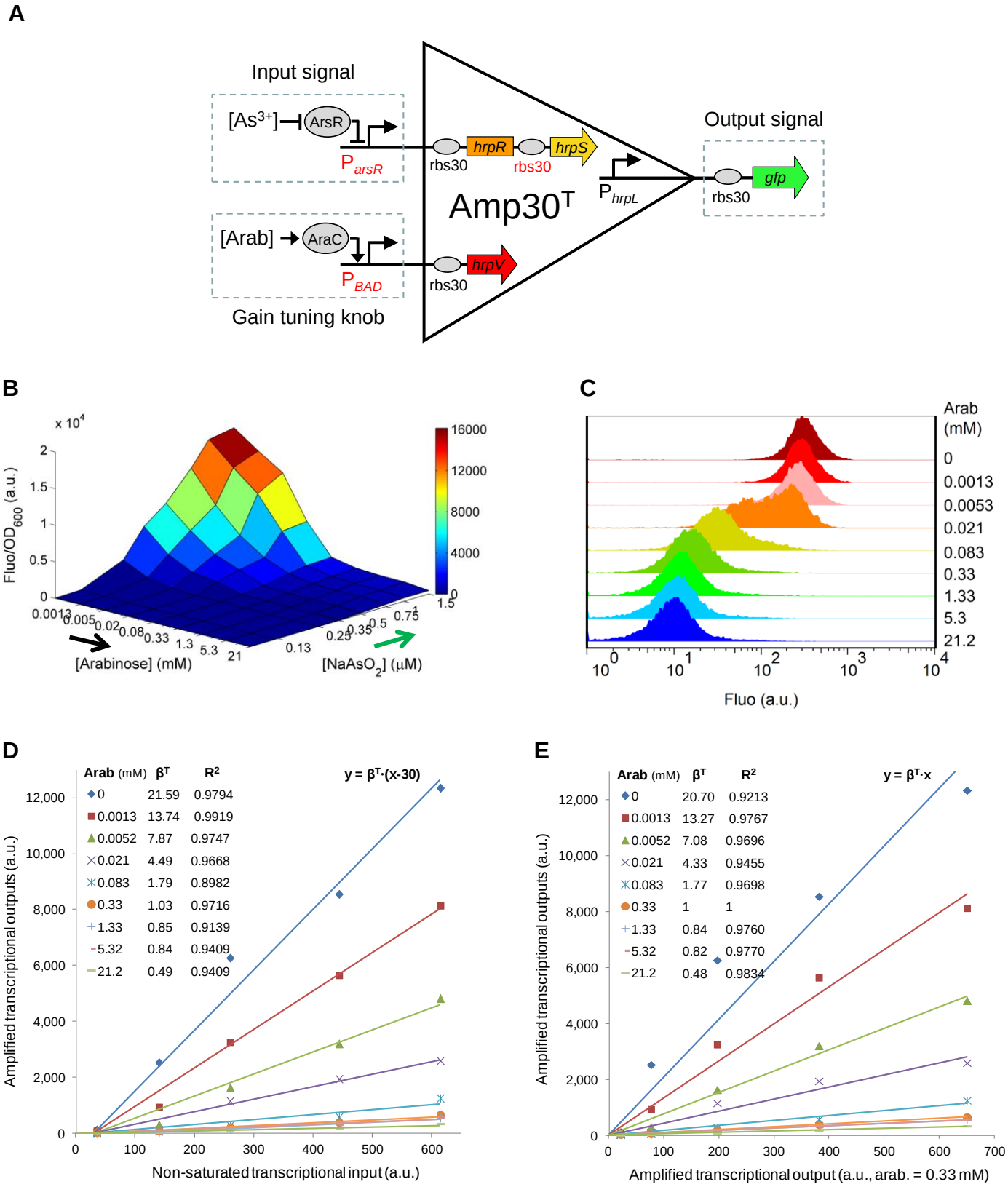

Figure S8: Engineering and characterization of the gain-tunable amplifier Amp30^T. (**A**) The architecture of the tunable amplifier Amp30^T which contains three terminals corresponding to the Signal input, Gain tuning knob and Signal output respectively. The arsenic sensor is connected to the first terminal as the input signal. The arabinose inducible promoter P_{BAD} is

connected to the second terminal to control the amplification gain while *gfp* as the output reporter. (**B**) Steady state response of the amplifier as in **a** under 72 combinations of two input inductions (0, 0.125, 0.25, 0.35, 0.5, 0.75, 1.0, 1.5 μM $NaAsO_2$ by 0, 1.3×10^{-3}, 5.2×10^{-3}, 2.1×10^{-2}, 8.3×10^{-2}, 0.33, 1.33, 5.32 and 21.2 mM arabinose) measured by fluorometry. Data are means and s.d. for three replicates. (**C**) The single cell flow cytometry data shows the cellular responses of the amplified arsenic sensor induced under 1.5 μM $NaAsO_2$ and varied arabinose concentrations. (**D**) Scatter plot showing the linearity between the non-saturated inputs and their amplified outputs of $Amp30^T$ under different gains as in **B** by fitting to a linear model. (**E**) Scatter plot showing the linearity between the amplified outputs of different gains as in **B**.

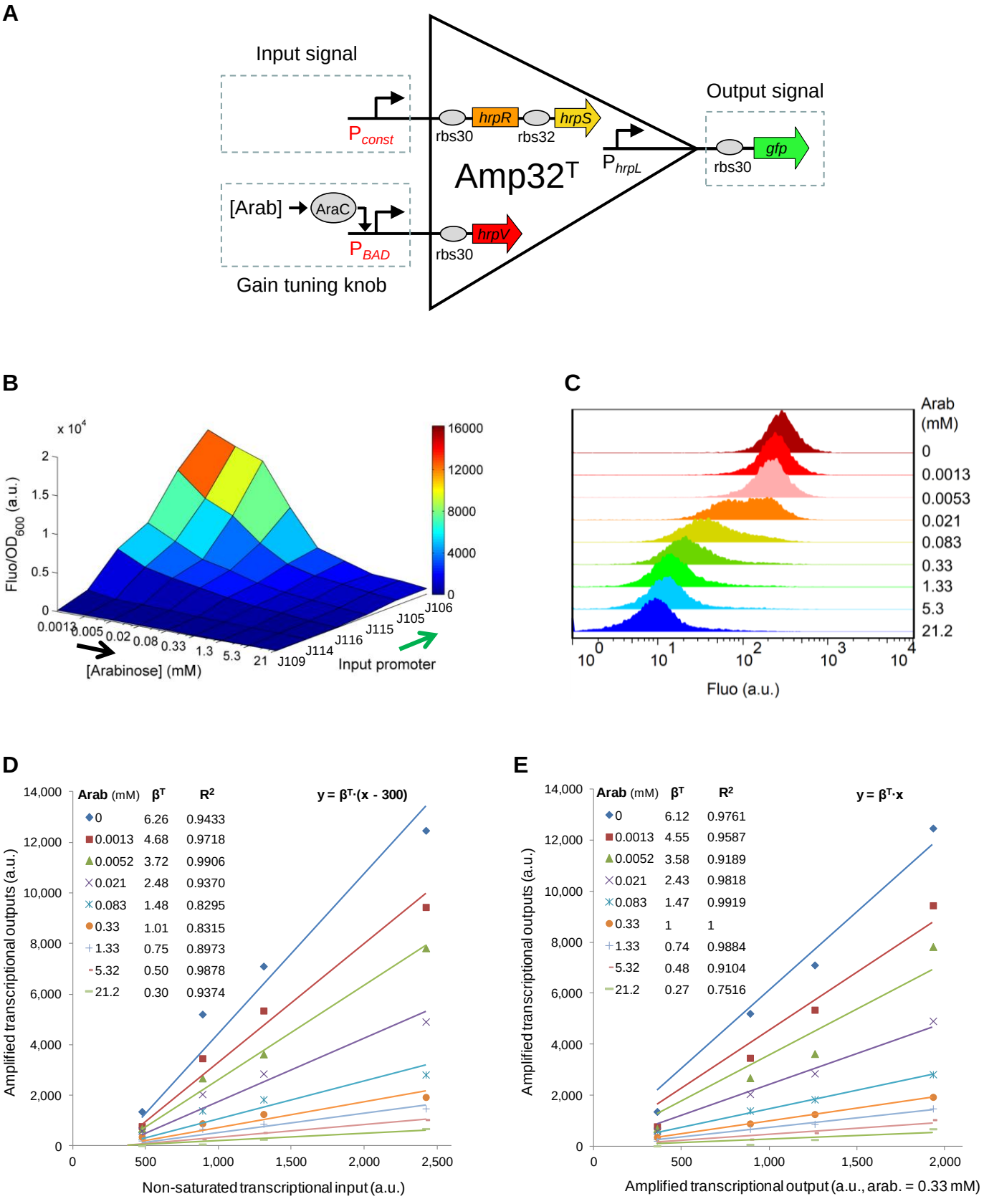

Figure S9: Engineering and characterization of the gain-tunable amplifier Amp32^{T}with alternate inputs. (**A**) The tunable amplifier Amp30^T comprises three terminals corresponding

to the Signal input, Gain tuning knob and Signal output respectively. Here, the arsenic sensor or a set of constitutive promoters is connected to the first terminal as the input signal. The arabinose inducible promoter P_{BAD} is connected to the second terminal to tune the amplification gain of the device while *gfp* is connected to the third terminal as output signal reporter. (**B**) Response of the amplifier with 6 constitutive promoters of incremental strengths as the input as in **a** under 54 two-input combinations (J109, J114, J116, J115, J105 and J106 by 0, 1.3×10^{-3}, 5.2×10^{-3}, 2.1×10^{-2}, 8.3×10^{-2}, 0.33, 1.33, 5.32 and 21.2 mM arabinose) measured by fluorometry. Data are means for three replicates. (**C**) The single cell flow cytometry data of the cellular responses of the amplifier with J106 as the signal input induced by differeent arabinose concentrations. (**E**) Scatter plot showing the linearity between the non-saturated inputs and their amplified outputs of $Amp32^{T}$ under different gains as in **B** by fitting to a linear model. (**E**) Scatter plot showing the linearity between the amplified outputs of different gains as in **B**.

A **B**

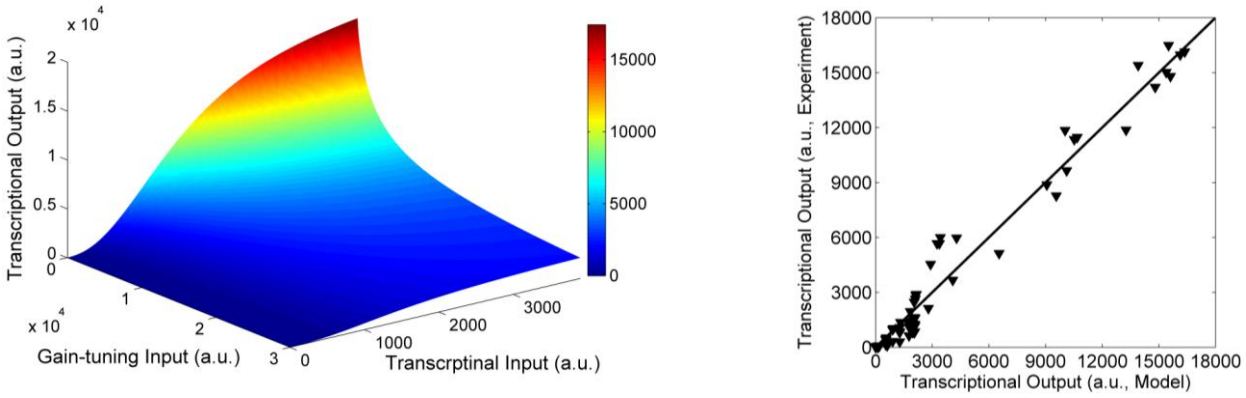

Figure S10: Amp32^T transfer function and comparison between model and experimental data. (**A**) The parameterised transfer function obtained by fitting to the experimental data (Fig. 4B, Table S2). (**B**) The Pearson correlation coefficients between the model and experimentally characterised responses of Amp32^T are 0.9863.

A **B**

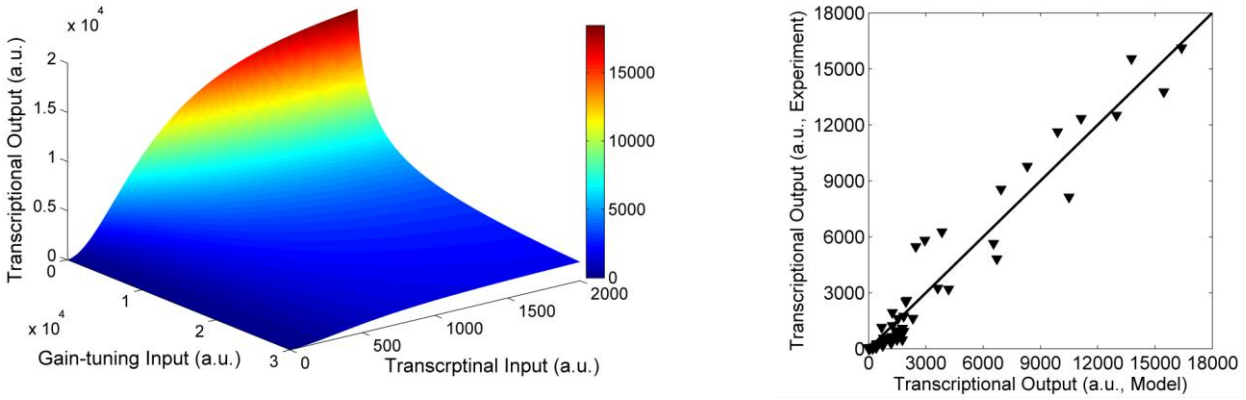

Figure S11: Amp30^T transfer function and comparison between model and experimental data. (**A**) The parameterised transfer function obtained by fitting to the experimental data (Fig. S8B, Table S2). (**B**) The Pearson correlation coefficients between the model and experimentally characterised responses of Amp30^T are 0.9736.

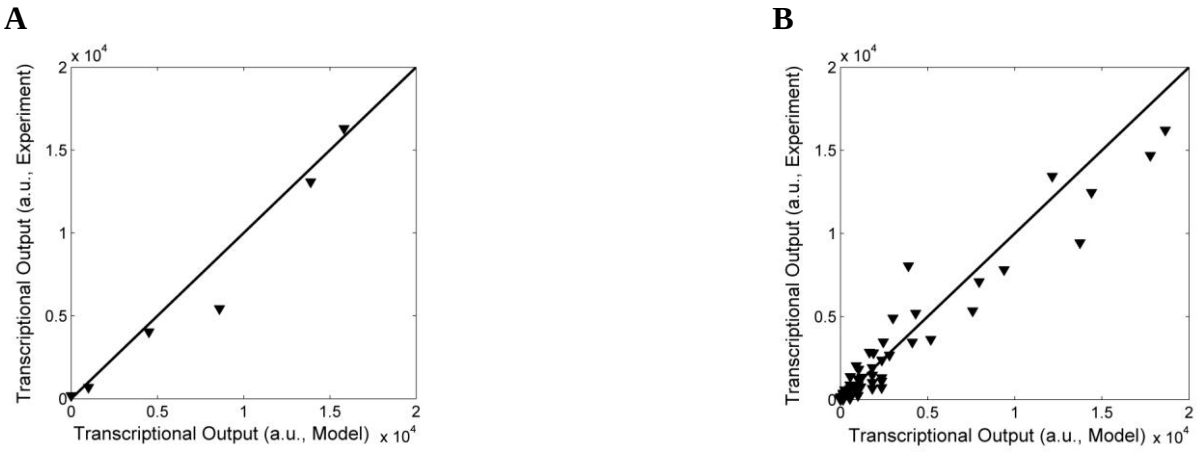

Figure S12: Comparison between amplifier model prediction and experimental data. (**A**) The Pearson correlation coefficient between the model predicted and experimentally characterised responses of the gain-fixed Amp32^{C} with the 6 constitutive promoters as inputs (Fig. 3D) is 0.9807. (**B**) The Pearson correlation coefficient between the model predicted and experimentally characterised responses of the gain-tunable Amp32^{T} with the 6 constitutive promoters as inputs (Fig. S9B) is 0.9643.

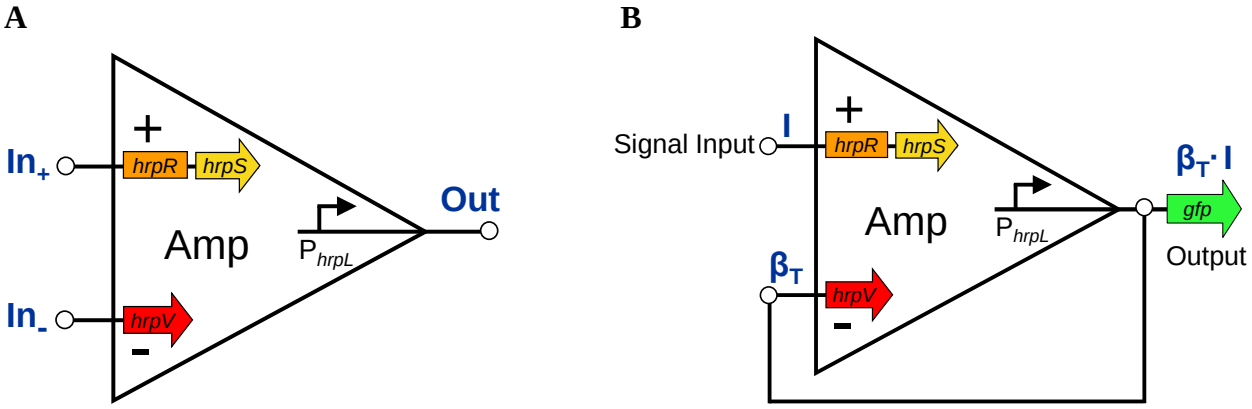

Figure S13: Schematics showing the potential applications of the tunable gain amplifier. (**A**) The device can be applied as a differential amplifier[2] (operational amplifier) with the output transcriptional signal is in proportion to the difference between the signal input and gain-tuning control input ($\Delta[Output] = a \cdot \Delta[In_+] - b \cdot \Delta[In_-]$). (**B**) The device can be potentially applied to construct a proportional negative feedback circuit to adaptively tune the output signal to stay at a constant level, thus exempted from the impact of environmental context variations on the signal input[3].

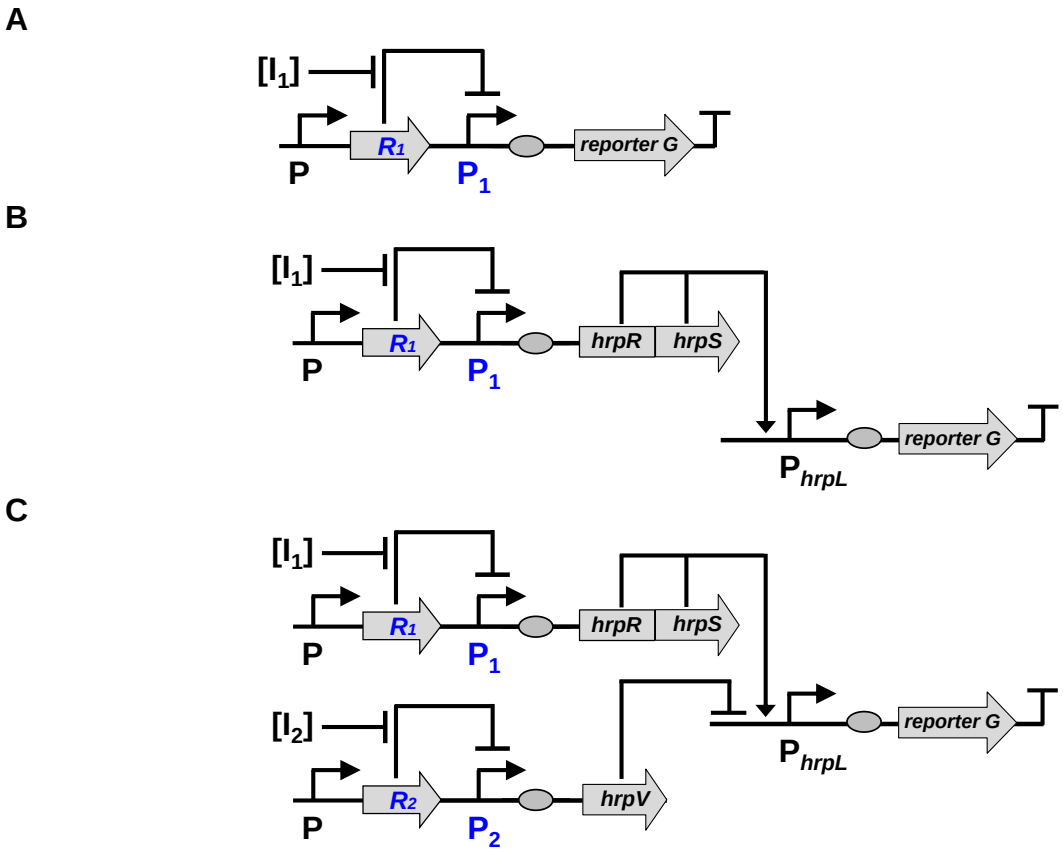

Figure S14: Schematics showing the architectures of the inducible negatively regulated promoter P_1 (A), the gain-fixed amplifier (B), and the gain-tunable amplifier (C).

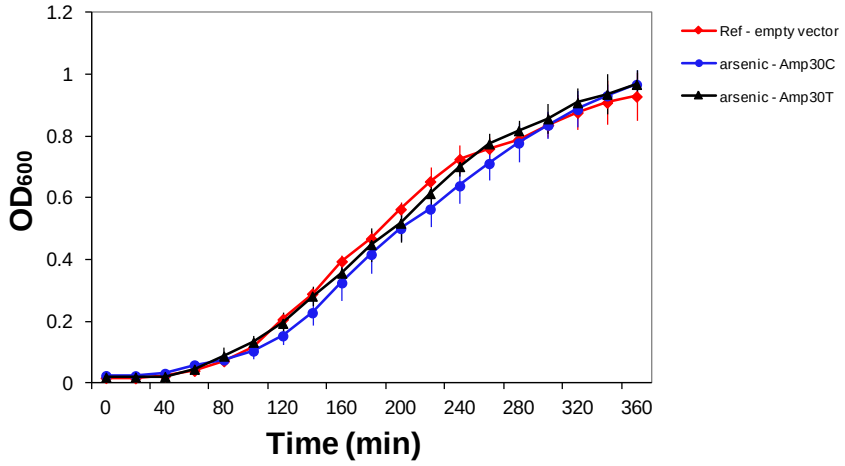

Figure S15: The growth curves of the genetic amplifiers ($Amp30^C$ and $Amp30^T$) engineered in this study compared to cells carrying the host plasmid alone show that the devices did not impose any observable growth burden on the *E. coli* host.

Host TOP10 cells containing various circuit constructs were used: one reference carrying the empty plasmid pSB3K3 alone (Ref – empty vectors), one carrying the plasmid with the functional $Amp30^C$ (pBW103ParsR-$Amp30^C$) using arsenic sensor as the input (Fig. 2, induced with 16 μM $NaAsO_2$), and one carrying the plasmid with the functional $Amp30^T$ (pBW301ParsR-$Amp30^T$) using arsenic sensor and P_{BAD} as the inputs (Fig. S8, induced with 16μM $NaAsO_2$ and 0.021 mM arabinose). The cells were grown in a 96 well microplate in fluorometer with shaking (200 rpm) for 6 hours. The absorbance (OD_{600}) was read every 20 min. The data were the average of three repeats from the three colonies of each strain. Cells were grown in LB media at 37 ℃. Error bars, s.d. (n = 3).

Supplementary Methods

Mathematical modelling and data fitting

Computational biochemical models were developed for individual genetic parts, and modules to abstract their behaviours for their future predictable assembly into larger synthetic biological systems. In this study, we focus on the average behaviour of the *E. coli* population to demonstrate the performance of the engineered circuits at steady state. First we used a simple linear mathematical formula ($y = k \cdot (x - b)$) to model the input-output relationship within the linear amplification dynamic range of the amplifier system. In addition, the ODEs-based deterministic model was used for accurately modelling the gene regulation and expression across the whole input or output range of the biochemical system. The following describes the derivation of the transfer function (TF) for each genetic circuit module and the experimental data fitting to these models.

1. Deriving transfer function of the inducible promoters

Figure S14A shows the exemplar architecture of the inducible promoter used in this study (*arsR*-P_{arsR} and *araC*-P_{BAD} promoters). The promoter P_1 is negatively regulated by its constitutively expressed repressor R_1 and is responsive to exogenous inducer I_1 to activate transcription of downstream reporter gene *G*. The reporter gene expression can be modelled by[4-6]:

$$\frac{d[G]}{dt} = \alpha \cdot k_1 + \frac{k_1 \cdot [I_1]^{n_1}}{[I_1]^{n_1} + K_1^{n_1}} - d \cdot [G] \quad \text{(S1)}$$

where $\alpha \cdot k_1$ is the basal constitutive activity of the promoter, $k_1 \cdot [I_1]^n / ([I_1]^n + K_1^n)$ is the activity due to cooperative transcription activation by assuming the concentration of the repressor is constant to model the effect of varying the concentration of the inducer I_1, and $d \cdot [G]$ is the constitutive degradation activity of protein G. K_1 and n_1 are the Hill constant and coefficient relating to the promoter-regulator/inducer interaction, k_1 is the maximum expression rate due to induction and α is a constant relating to the promoter basal level due to leakage ($0 \leq \alpha < 1$), and d is the degradation rate of G.

The steady state solution of equation S1 is given by

$$f([I_1]) = [G]_{ss} = k \cdot (\alpha + [I_1]^{n_1} / (K_1^{n_1} + [I_1]^{n_1})) \quad \text{(S2)}$$

in which $k = k_1/d$ represents the maximum expression level due to induction. Equation S2 gives the reporter protein level at steady state for the inducible promoter P_1 and is also the TF of P_1. We used this TF to fit the characterisation data of the arsenite (Fig. S1) and arabinose (Fig. S4) inducible promoters using the nonlinear least square fitting function in Matlab. The best fit coefficients (with 95% confidence bounds otherwise fixed at bound) are listed in Supplementary Table S1 and the parameterised TFs are plotted in Fig. S1B and Fig. S2B respectively against their experimental data.

2. Deriving transfer function of the gain-fixed amplifier (Amp^C)

Figure S14B shows the architecture of the gain-fixed amplifier in this study. *hrpL* promoter is synergistically activated by the heteromeric protein complex HrpRS, which are co-transcribed as a single operon. Based on the known mechanism underlying this hetero-regulated module[6-7], the two bacterial enhancer-binding proteins form an active hetero-hexamer complex first to bind the UAS (upstream activation sequence) of *hrpL* to remodel the conformation of σ^{54}-RNAP-*hrpL* close promoter complex to an open one for the transcriptional activation. The amplifier TF can be described by the following Hill function curve with quasi-stationary approximation:

$$f([RS]_{ss}) = k_C \cdot \frac{([RS]_{ss}/K_{RS})^{n_{RS}}}{1+([RS]_{ss}/K_{RS})^{n_{RS}}} \quad \text{(S3)}$$

in which K_{RS} and n_{RS} are the Hill constant and coefficient for HrpRS co-activator. $[RS]_{ss}$ is the steady level of HrpRS, whose level is under the control of the inducible promoter P_1 as indicated by equation S2 or a constitutive promoter. k_C is the maximum output level of the amplifier at steady state.

The TF was parameterised by fitting to the experimental data of the two amplifiers $Amp32^C$ and $Amp30^C$ (Fig. 2B). The best fit coefficients by nonlinear least square optimisation were obtained as shown in Supplementary Table S2. The parametrised TFs are plotted in Fig. S2B and Fig. S3B respectively against the experimental data. Figure S12A shows the linear correlation between predicted and experimentally characterised responses of the amplifier with alternate constitutive promoter inputs (Fig. 3D).

3. Deriving transfer function of the gain-tunable amplifier (Amp^T)

Figure S14C shows the architecture of the gain-tunable genetic amplifier in this study. The device is designed on the basis of the three regulatory components HrpR, HrpS, HrpV and one output regulated promoter *hrpL*. The *hrpL* promoter is activated by the heteromeric protein complex HrpRS, transcribed from a single operon, while negatively regulated by the HrpV protein through a direct interaction with HrpS[7-8]. As shown, the amplifier can be characterised under two inducible promoters P_1 (in response to inducer I_1) as the input signal and P_2 (in response to inducer I_2) as the gain tuning input. Following quasi-stationary approximation, the device TF can be modelled by

$$f([RS]_{ss},[V]_{SS}) = k_T \cdot \frac{([RS]_{ss}/K_{RS})^{n_{RS}}}{1+([RS]_{ss}/K_{RS})^{n_{RS}}} \cdot \frac{1}{1+([V]_{ss}/K_V)^{n_V}} \quad \text{(S4)}$$

in which K_{RS} and n_{RS} are the Hill constant and coefficient for HrpRS co-activator. $[RS]_{ss}$ is the steady level of HrpRS, whose level is under the control of the inducible promoters P_1 as indicated by equation S2 or a constitutive promoter. K_V and n_V are the Hill constant and coefficient for HrpV repressor. $[V]_{ss}$ is the steady level of HrpV, whose level is under the control of the inducible promoter P_2 as indicated by equation S2. k_T is the maximum output level of the amplifier at steady state.

The characterisation data of the Amp32^T and Amp30^T using arsenic sensor as the signal input and P_{BAD} promoter as the gain-tuning input (Fig. 4B, Figure S8B) were fitted to this transfer function model and the results are listed in Supplementary Table S2. The parametrised TFs are plotted in Fig. S10A and Fig. S11A respectively. There are high linear correlation between model prediction and the experimental data as shown in Fig. S10B and Fig. S11B. Figure S12B show the linear correlation between the model predicted and experimentally characterised responses of the amplifier Amp32^T with alternate constitutive promoter inputs (Fig. S9B).

4. Deriving device linear dynamic range

The device linear dynamic range in Figure S2B and S3B is derived according to the difference (non-linearity) between the fitted Hill function and the fitted linear function for the experimental characterisation data. If non-linearity |(Hill (x) – Linear (x))/Linear (x)| <=15%, the corresponding transcriptional input (x) and output (Linear (x)) is considered within the device's input and output linear dynamic ranges.

Table S1: The best fits of the characterised promoter responses. Data shown are with 95% confidence bounds.

Promoter Input	k (a.u.)	n_1	K_1 (μM)	α	R^2
P_{J101}-rbs32-*arsR*-B0015-P_{arsR}	3235 ± 146	1.332 ± 0.171	2.088 ± 0.299	5.069e-10	0.9972
araC-P_{BAD}	2.801e4 ± 0.069e4	2.195 ± 0.62	21.82 ± 2.07	3.823e-9	0.9985

Table S2: The best fits for the characterised responses of the amplifiers. Data shown are with 95% confidence bounds.

Amplifier	k_C or k_T (a.u.)	n_{RS}	K_{RS} (a.u.)	n_V	K_V (a.u.)	R^2
$Amp32^C$	1.602e4 ± 0.135e4	2.811 ± 0.62	1243 ± 141	N/A	N/A	0.9964
$Amp30^C$	1.534e4 ± 0.083e4	1.715 ± 0.393	326.1 ± 49.8	N/A	N/A	0.9932
$Amp32^T$	1.95e4 ± 0.317e4	2.295 ± 0.618	1540 ± 296	0.8003 ± 0.0917	2528 ± 620	0.9725
$Amp30^T$	2.039e4 ± 0.513e4	1.876 ± 0.572	600.5 ± 199.3	0.7936 ± 0.1443	1961 ± 777	0.9468

Table S3: Amp32^{T} (P_{arsR} as signal input and P_{BAD} as gain tuning input, Fig. 4B, D, E) linear correlation coefficient matrix between the unsaturated input and the outputs under different gains (indicated by varying arabinose concentrations)

		Input	Amp32^{T} Outputs (Arabinose - mM)								
			0	1.3×10^{-3}	5.2 ×10^{-3}	2.1 ×10^{-2}	8.3 ×10^{-2}	0.33	1.33	5.32	21.2
	Input	1	0.9983	0.9998	0.9893	0.9885	0.9987	0.9985	0.9985	0.9969	0.9658
Outputs (Arabinose - mM)	0	0.9983	1	0.997	0.9796	0.978	0.9944	0.9991	0.9957	0.9985	0.951
	1.3×10^{-3}	0.9998	0.997	1	0.992	0.9913	0.9991	0.9972	0.999	0.9959	0.9708
	5.2 ×10^{-3}	0.9893	0.9796	0.992	1	0.9996	0.9925	0.9802	0.993	0.9812	0.9929
	2.1 ×10^{-2}	0.9885	0.978	0.9913	0.9996	1	0.993	0.9799	0.991	0.9783	0.9916
	8.3 ×10^{-2}	0.9987	0.9944	0.9991	0.9925	0.993	1	0.9964	0.9966	0.9916	0.9709
	0.33	0.9985	0.9991	0.9972	0.9802	0.9799	0.9964	1	0.9943	0.9956	0.9504
	1.33	0.9985	0.9957	0.999	0.993	0.991	0.9966	0.9943	1	0.9972	0.975
	5.32	0.9969	0.9985	0.9959	0.9812	0.9783	0.9916	0.9956	0.9972	1	0.9569
	21.2	0.9658	0.951	0.9708	0.9929	0.9916	0.9709	0.9504	0.975	0.9569	1

Table S4: *p*-values of Amp32^{T} (P_{arsR} as signal input and P_{BAD} as gain tuning input, Fig. 4B, D, E) linear correlation coefficient matrix between the unsaturated input and the outputs under different gains (indicated by varying arabinose concentrations)

		Input	Amp32^{T} Outputs (Arabinose - mM)								
			21.2	5.32	1.33	0.33	8.3 ×10^{-2}	2.1 ×10^{-2}	5.2 ×10^{-3}	1.3×10^{-3}	0
	Input	0	0.0017	0.0002	0.0107	0.0115	0.0013	0.0015	0.0015	0.0031	0.0342
Outputs (Arabinose - mM)	21.2	0.0017	0	0.0030	0.0204	0.0220	0.0056	0.0009	0.0043	0.0015	0.0491
	5.32	0.0002	0.0030	0	0.0080	0.0087	0.0009	0.0028	0.0010	0.0041	0.0292
	1.33	0.0107	0.0204	0.0080	0	0.0004	0.0075	0.0198	0.0070	0.0188	0.0071
	0.33	0.0115	0.0220	0.0087	0.0004	0	0.0070	0.0201	0.0090	0.0217	0.0084
	8.3 ×10^{-2}	0.0013	0.0056	0.0009	0.0075	0.0070	0	0.0036	0.0034	0.0084	0.0291
	2.1 ×10^{-2}	0.0015	0.0009	0.0028	0.0198	0.0201	0.0036	0	0.0057	0.0044	0.0496
	5.2 ×10^{-3}	0.0015	0.0043	0.0010	0.0070	0.0090	0.0034	0.0057	0	0.0028	0.0250
	1.3×10^{-3}	0.0031	0.0015	0.0041	0.0188	0.0217	0.0084	0.0044	0.0028	0	0.0431
	0	0.0342	0.0491	0.0292	0.0071	0.0084	0.0291	0.0496	0.0250	0.0431	0

Table S5: Amp30^T (P_{arsR} as signal input and P_{BAD} as gain tuning input, Fig. S5B, D, E) linear correlation coefficient matrix between the unsaturated input and the outputs under different gains (indicated by varying arabinose concentrations)

		Input	Amp30^T Outputs (Arabinose - mM)								
			0	1.3×10^{-3}	5.2 ×10^{-3}	2.1 ×10^{-2}	8.3 ×10^{-2}	0.33	1.33	5.32	21.2
	Input	1	0.9915	0.997	0.9928	0.9859	0.9628	0.988	0.9843	0.9708	0.9726
Outputs (Arabinose - mM)	0	0.9915	1	0.9916	0.9815	0.9852	0.9455	0.973	0.9633	0.946	0.9516
	1.3×10^{-3}	0.997	0.9916	1	0.9977	0.9948	0.9657	0.989	0.9892	0.9705	0.9742
	5.2 ×10^{-3}	0.9928	0.9815	0.9977	1	0.9917	0.9759	0.9937	0.9966	0.9807	0.9838
	2.1 ×10^{-2}	0.9859	0.9852	0.9948	0.9917	1	0.9433	0.9725	0.9806	0.9476	0.9535
	8.3 ×10^{-2}	0.9628	0.9455	0.9657	0.9759	0.9433	1	0.9927	0.9813	0.9967	0.9982
	0.33	0.988	0.973	0.989	0.9937	0.9725	0.9927	1	0.994	0.9951	0.9966
	1.33	0.9843	0.9633	0.9892	0.9966	0.9806	0.9813	0.994	1	0.9884	0.9897
	5.32	0.9708	0.946	0.9705	0.9807	0.9476	0.9967	0.9951	0.9884	1	0.9994
	21.2	0.9726	0.9516	0.9742	0.9838	0.9535	0.9982	0.9966	0.9897	0.9994	1

Table S6: Amp32^T (P_C as signal input and P_{BAD} as gain tuning input, Fig. S6 B, D, E) linear correlation coefficient matrix between the unsaturated input and the outputs under different gains (indicated by varying arabinose concentrations)

		Input	Amp32^T Outputs (Arabinose - mM)								
			0	1.3×10^{-3}	5.2 ×10^{-3}	2.1 ×10^{-2}	8.3 ×10^{-2}	0.33	1.33	5.32	21.2
	Input	1.0000	0.9882	0.9914	0.9966	0.9891	0.9695	0.9838	0.9847	0.9969	0.9920
Outputs (Arabinose - mM)	0	0.9882	1.0000	0.9989	0.9924	0.9999	0.9952	0.9977	0.9997	0.9755	0.9614
	1.3×10^{-3}	0.9914	0.9989	1.0000	0.9916	0.9995	0.9929	0.9987	0.9976	0.9823	0.9692
	5.2 ×10^{-3}	0.9966	0.9924	0.9916	1.0000	0.9920	0.9757	0.9841	0.9907	0.9871	0.9806
	2.1 ×10^{-2}	0.9891	0.9999	0.9995	0.9920	1.0000	0.9950	0.9984	0.9993	0.9775	0.9635
	8.3 ×10^{-2}	0.9695	0.9952	0.9929	0.9757	0.9950	1.0000	0.9966	0.9964	0.9530	0.9329
	0.33	0.9838	0.9977	0.9987	0.9841	0.9984	0.9966	1.0000	0.9969	0.9734	0.9573
	1.33	0.9847	0.9997	0.9976	0.9907	0.9993	0.9964	0.9969	1.0000	0.9702	0.9551
	5.32	0.9969	0.9755	0.9823	0.9871	0.9775	0.9530	0.9734	0.9702	1.0000	0.9980
	21.2	0.9920	0.9614	0.9692	0.9806	0.9635	0.9329	0.9573	0.9551	0.9980	1.0000

Table S7. List of genetic parts used in this study.

Part name	Type and source	DNA sequence (5′ – 3′)
hrpR	Gene[6,9]	ATGAGTACAGGCATCGATAAGGACGTCCGAGAGTGTTGGGGCGTAACTGCAT TATCAGCGGGTCATCAAATTGCAATGAATAGCGCGTTTCTGGATATGGACTT GCTGTTGTGCGGGGAAACCGGCACCGGCAAGGACACACTGGCCAACCGCATT CACGAGTTGTCCAGCAGGTCGGGACCCTTTGTGGGCATGAACTGCGCCGCCA TTCCCGAGTCGCTGGCAGAGAGCCAGTTATTCGGTGTGGTCAACGGTGCATT CACCGGCGTATGCCGGGCTCGCGAGGGCTACATAGAGGCCTCCAGTGGTGGC ACCTTGTACCTGGATGAAATCGACAGCATGCCGTTGAGCCTGCAAGCCAAAC TGCTGCGTGTGTTGGAGAGTCGAGGTATCGAGCGTCTGGGCTCGACCGAATT TATCCCGGTGGATCTGCGGATCATTGCCTCGGCCCAGCGGCCACTGGATGAA CTGGTGGAACAAGGACTTTTCCGTCGCGACCTGTTTTTTCGGCTCAACGTGC TGACGCTTCACTTGCCAGCCTTGCGCAAACGTCGTGAACAGATCCTGCCATT GTTCGACCAGTTCACCCAGGGTATCGCTGCCGAGTTCGGACGTCCCGCTCCT GCGCTGGACAGCGGGCGTGTGCAGCTGCTGCTCAGCCACGACTGGCCGGGCA ACATCCGCGAATTGAAGTCTGCGGCCAAGCGCTTCGTACTCGGCTTCCCCTT GCTGGGCGCCGACCCTGTGGAAGCGCTTGACCCTGCCACGGGGCTGCGCACG CAAATGCGCATCATCGAGAAAATGCTCATCCAGGATGCCTTGAAGCGGCACA GGCACAATTTCGACGCGGTGCTTCAGGAGTTGGAGTTGCCAAGACGCACCCT GTATCACCGCATGAAGGAACTGGGAGTTGCAGCGCCGATCGCTGCGACGGCC GGGGTCTAATAA
hrpS	Gene[6,9]	ATGAGTCTTGATGAAAGGTTTGAGGATGATCTGGACGAGGAGCGGGTTCCGA ATCTGGGGATAGTTGCCGAAAGTATTTCGCAACTGGGTATCGACGTGCTGCT ATCGGGTGAGACCGGCACGGGCAAAGACACGATTGCCCGACGGATTCATGAG ATGTCAGGCCGCAAAGGGCGCCTGGTGGCGATGAATTGCGCGGCCATTCCGG AGTCCCTCGCCGAGAGCGAGTTATTCGGCGTGGTCAGCGGTGCCTACACCGG CGCTGATCGCTCCAGAGTCGGTTATGTCGAAGCGGCGCAGGGCGGCACGCTG TACCTGGATGAGATCGATAGCATGCCGCTGAGCCTGCAAGCCAAATTGCTGA GGGTGCTGGAAACCCGAGCGCTTGAACGGCTGGGTTCGACGTCGACGATCAA GCTGGATATCTGCGTGATCGCCTCCGCCCAATGCTCGCTGGACGACGCCGTC GAGCGGGGGCAGTTTCGTCGCGATCTGTATTTTCGCCTGAACGTCCTGACAC TCAAGCTTCCTCCGCTACGTAACCAGTCTGATCGCATAGTTCCCCTGTTCAC ACGTTTTACGGCCGCCGCCGCGAGGGAGCTCGGTGTTCCCGTTCCCGATGTT TGCCCACTGCTGCACAAAGTGCTGCTGGGCCACGACTGGCCCGGCAATATCC GTGAGCTCAAGGCGGCAGCCAAACGCCATGTGCTGGGTTTCCCCTTGCTGGG CGCCGAGCCGCAGGGCGAAGAGCACTTGGCCTGTGGGCTCAAATCGCAATTG CGAGTGATCGAAAAAGCCCTGATTCAGGAGTCGCTCAAGCGCCACGACAATT GTGTGGATTCGGTAAGCCTGGAACTGGACGTGCCACGCCGTACGCTCTATCG ACGCATCAAAGAATTGCAGATCTAATAA
hrpV	Gene[8-9]	ATGATTGAGGTAACGGAAAAGTCGGCATTTTACGCTCAGGTTGCCGCCCAGA GCCCAGCAGTATGGCCAGTGGCCAATGGCGTCGCGTTTGTCAGTCGGCGCGA ACACCATGATTGGGGGATCGCCTTGCACATAGAAGGCCGCGCGTTGCGTCCC GATCAACTGCGTGATGCACTGCAACGACGTTTTATGGAGTCAGAGCGTTTCA ATCACTACTTCCTGTTTCTGGACGTACGACGCGACTTTGTGGTGTGGCACGC GGTCAACGAAAAACCGGGTTCCTACGCCAGCCTGGACGACATCCGCCGGCAT GAGTTGATGCTGGCAGGGCTGGACCATTTGAGCGAGGAAATGCACTAATAA
hrpL	Promoter[6,9]	GCCGGATTATGTCCGCTGAGTGGGTCACGGTCCCGGATCAGTTCCCTTGCGA AGCTGACCGATGTTTTTGTGCCAAAAGCTGTTGTGGCAAAAAACGGTTTGCG CAAAGTTTTGTATTACAAAGAATTTCACATTTTAAAATATCTTTATAAATCA ATCAGTTATTTCTATTTTTAAGCTGGCATGGTTATCGCTATAGGGCTTGTAC

P_{J101}-rbs32-arsR-B0015-P_{arsR}	Inducible Promoter[10] (de novo synthesized)	TTTACAGCTAGCTCAGTCCTTGGTATTATGCTAGCTCCTAGGGTCACACAGG AAAGTACCATATGTCATTTCTGTTACCCATCCAATTGTTCAAAATTCTTGCT GATGAAACCCGTCTGGGCATCGTTTTACTGCTCAGCGAACTGGGAGAGTTAT GCGTCTGCGATCTCTGCACTGCTCTCGACCAGTCGCAGCCCAAGATCTCCCG CCACCTGGCATTGCTGCGTGAAAGCGGGCTATTGCTGGACCGCAAGCAAGGT AAGTGGGTTCATTACCGCTTATCACCGCATATTCCAGCATGGGCGGCGAAAA TTATTGATGAGGCCTGGCGATGTGAACAGGAAAAGGTTCAGGCGATTGTCCG CAACCTGGCTCGACAAAACTGTTCCGGGGACAGTAAGAACATTTGCAGTTAA AAATTTAGCTAAACACACATGAATTTTCAGATGTGTTTTATCCGGGTACTAG AGCCAGGCATCAAATAAAACGAAAGGCTCAGTCGAAAGACTGGGCCTTTCGT TTTATCTGTTGTTTGTCGGTGAACGCTCTCTACTAGAGTCACACTGGCTCAC CTTCGGGTGGGCCTTTCTGCGTTTATATACTAGAGCCAACTCAAAATTCACA CCTATTACCTTCCTCTGCACTTACACATTCGTTAAGTCATATATGTTTTTGA CTTATCCGCTTCGAAGAGAGACACTACCTGCAA
araC-P_{BAD}	Inducible Promoter[11]	TTATGACAACTTGACGGCTACATCATTCACTTTTTCTTCACAACCGGCACGG AACTCGCTCGGGCTGGCCCCGGTGCATTTTTTAAATACCCGCGAGAAATAGA GTTGATCGTCAAAACCAACATTGCGACCGACGGTGGCGATAGGCATCCGGGT GGTGCTCAAAAGCAGCTTCGCCTGGCTGATACGTTGGTCCTCGCGCCAGCTT AAGACGCTAATCCCTAACTGCTGGCGGAAAAGATGTGACAGACGCGACGGCG ACAAGCAAACATGCTGTGCGACGCTGGCGATATCAAAATTGCTGTCTGCCAG GTGATCGCTGATGTACTGACAAGCCTCGCGTACCCGATTATCCATCGGTGGA TGGAGCGACTCGTTAATCGCTTCCATGCGCCGCAGTAACAATTGCTCAAGCA GATTTATCGCCAGCAGCTCCGAATAGCGCCCTTCCCCTTGCCCGGCGTTAAT GATTTGCCCAAACAGGTCGCTGAAATGCGGCTGGTGCGCTTCATCCGGGCGA AAGAACCCCGTATTGGCAAATATTGACGGCCAGTTAAGCCATTCATGCCAGT AGGCGCGCGGACGAAAGTAAACCCACTGGTGATACCATTCGCGAGCCTCCGG ATGACGACCGTAGTGATGAATCTCTCCTGGCGGGAACAGCAAAATATCACCC GGTCGGCAAACAAATTCTCGTCCCTGATTTTTCACCACCCCCTGACCGCGAA TGGTGAGATTGAGAATATAACCTTTCATTCCCAGCGGTCGGTCGATAAAAAA ATCGAGATAACCGTTGGCCTCAATCGGCGTTAAACCCGCCACCAGATGGGCA TTAAACGAGTATCCCGGCAGCAGGGGATCATTTTGCGCTTCAGCCATACTTT TCATACTCCCGCCATTCAGAGAAGAAACCAATTGTCCATATTGCATCAGACA TTGCCGTCACTGCGTCTTTTACTGGCTCTTCTCGCTAACCAAACCGGTAACC CCGCTTATTAAAAGCATTCTGTAACAAAGCGGGACCAAAGCCATGACAAAAA CGCGTAACAAAAGTGTCTATAATCACGGCAGAAAAGTCCACATTGATTATTT GCACGGCGTCACACTTTGCTATGCCATAGCATTTTTATCCATAAGATTAGCG GATCCTACCTGACGCTTTTTATCGCAACTCTC**TACTGT**TTCTCCAT
rbs30	RBS[3]	TCTAGAGATTAAAGAGGAGAAATACTAGATG
rbs32	RBS[3]	TCTAGAGTCACACAGGAAAGTACTAGATG
J109	Promoter[12]	TTTACAGCTAGCTCAGTCCTAGGGACTGTGCTAGC
J114	Promoter[12]	TTTATGGCTAGCTCAGTCCTAGGTACAATGCTAGC
J116	Promoter[12]	TTGACAGCTAGCTCAGTCCTAGGGACTATGCTAGC
J115	Promoter[12]	TTTATAGCTAGCTCAGCCCTTGGTACAATGCTAGC
J105	Promoter[12]	TTTACGGCTAGCTCAGTCCTAGGTACTATGCTAGC
J106	Promoter[12]	TTTACGGCTAGCTCAGTCCTAGGTATAGTGCTAGC
B0015 (B15)	Terminator[13]	CCAGGCATCAAATAAAACGAAAGGCTCAGTCGAAAGACTGGGCCTTTCGTTT TATCTGTTGTTTGTCGGTGAACGCTCTCTACTAGAGTCACACTGGCTCACCT TCGGGTGGGCCTTTCTGCGTTTATA

gfp	Gene[3,14]	ATGCGTAAAGGAGAAGAACTTTTCACTGGAGTTGTCCCAATTCTTGTTGAAT TAGATGGTGATGTTAATGGGCACAAATTTTCTGTCAGTGGAGAGGGTGAAGG TGATGCAACATACGGAAAACTTACCCTTAAATTTATTTGCACTACTGGAAAA CTACCTGTTCCATGGCCAACACTTGTCACTACTTTCGGTTATGGTGTTCAAT GCTTTGCGAGATACCCAGATCATATGAAACAGCATGACTTTTTCAAGAGTGC CATGCCCGAAGGTTATGTACAGGAAAGAACTATATTTTTCAAAGATGACGGG AACTACAAGACACGTGCTGAAGTCAAGTTTGAAGGTGATACCCTTGTTAATA GAATCGAGTTAAAAGGTATTGATTTTAAAGAAGATGGAAACATTCTTGGACA CAAATTGGAATACAACTATAACTCACACAATGTATACATCATGGCAGACAAA CAAAAGAATGGAATCAAAGTTAACTTCAAAATTAGACACAACATTGAAGATG GAAGCGTTCAACTAGCAGACCATTATCAACAAAATACTCCAATTGGCGATGG CCCTGTCCTTTTACCAGACAACCATTACCTGTCCACACAATCTGCCCTTTCG AAAGATCCCAACGAAAAGAGAGACCACATGGTCCTTCTTGAGTTTGTAACAG CTGCTGGGATTACACATGGCATGGATGAACTATACAAATAATAA
pSB3K3	Plasmid backbone[15-16]	TACTAGTAGCGGCCGCTGCAGTCCGGCAAAAAAACGGGCAAGGTGTCACCACCCTGCC CTTTTTCTTTAAAACCGAAAAGATTACTTCGCGTTATGCAGGCTTCCTCGCTCACTGA CTCGCTGCGCTCGGTCGTTCGGCTGCGGCGAGCGGTATCAGCTCACTCAAAGGCGGTA ATCTCGAGTCCCGTCAAGTCAGCGTAATGCTCTGCCAGTGTTACAACCAATTAACCAA TTCTGATTAGAAAAACTCATCGAGCATCAAATGAAACTGCAATTTATTCATATCAGGA TTATCAATACCATATTTTTGAAAAAGCCGTTTCTGTAATGAAGGAGAAAACTCACCGA GGCAGTTCCATAGGATGGCAAGATCCTGGTATCGGTCTGCGATTCCGACTCGTCCAAC ATCAATACAACCTATTAATTTCCCCTCGTCAAAAATAAGGTTATCAAGTGAGAAATCA CCATGAGTGACGACTGAATCCGGTGAGAATGGCAAAAGCTTATGCATTTCTTTCCAGA CTTGTTCAACAGGCCAGCCATTACGCTCGTCATCAAAATCACTCGCATCAACCAAACC GTTATTCATTCGTGATTGCGCCTGAGCGAGACGAAATACGCGATCGCTGTTAAAAGGA CAATTACAAACAGGAATCGAATGCAACCGGCGCAGGAACACTGCCAGCGCATCAACAA TATTTTCACCTGAATCAGGATATTCTTCTAATACCTGGAATGCTGTTTTCCCGGGGAT CGCAGTGGTGAGTAACCATGCATCATCAGGAGTACGGATAAAATGCTTGATGGTCGGA AGAGGCATAAATTCCGTCAGCCAGTTTAGTCTGACCATCTCATCTGTAACATCATTGG CAACGCTACCTTTGCCATGTTTCAGAAACAACTCTGGCGCATCGGGCTTCCCATACAA TCGATAGATTGTCGCACCTGATTGCCCGACATTATCGCGAGCCCATTTATACCCATAT AAATCAGCATCCATGTTGGAATTTAATCGCGGCCTCGAGCAAGACGTTTCCCGTTGAA TATGGCTCATAACACCCCTTGTATTACTGTTTATGTAAGCAGACAGTTTTATTGTTCA TGATGATATATTTTTATCTTGTGCAATGTAACATCAGAGATTTTGAGACACAACGTGG CTTTGTTGAATAAATCGAACTTTTGCTGAGTTGAAGGATCAGATCACGCATCTTCCCG ACAACGCAGACCGTTCCGTGGCAAAGCAAAAGTTCAAAATCACCAACTGGTCCACCTA CAACAAAGCTCTCATCAACCGTGGCTCCCTCACTTTCTGGCTGGATGATGGGGCGATT CAGGCCTGGTATGAGTCAGCAACACCTTCTTCACGAGGCAGACCTCAGCGCTAGCGGA GTGTATACTGGCTTACTATGTTGGCACTGATGAGGGTGTCAGTGAAGTGCTTCATGTG GCAGGAGAAAAAAGGCTGCACCGGTGCGTCAGCAGAATATGTGATACAGGATATATTC CGCTTCCTCGCTCACTGACTCGCTACGCTCGGTCGTTCGACTGCGGCGAGCGGAAATG GCTTACGAACGGGGCGGAGATTTCCTGGAAGATGCCAGGAAGATACTTAACAGGGAAG TGAGAGGGCCGCGGCAAAGCCGTTTTTCCATAGGCTCCGCCCCCCTGACAAGCATCAC GAAATCTGACGCTCAAATCAGTGGTGGCGAAACCCGACAGGACTATAAAGATACCAGG CGTTTCCCCTGGCGGCTCCCTCGTGCGCTCTCCTGTTCCTGCCTTTCGGTTTACCGGT GTCATTCCGCTGTTATGGCCGCGTTTGTCTCATTCCACGCCTGACACTCAGTTCCGGG TAGGCAGTTCGCTCCAAGCTGGACTGTATGCACGAACCCCCCGTTCAGTCCGACCGCT GCGCCTTATCCGGTAACTATCGTCTTGAGTCCAACCCGGAAAGACATGCAAAAGCACC ACTGGCAGCAGCCACTGGTAATTGATTTAGAGGAGTTAGTCTTGAAGTCATGCGCCGG TTAAGGCTAAACTGAAAGGACAAGTTTTGGTGACTGCGCTCCTCCAAGCCAGTTACCT CGGTTCAAAGAGTTGGTAGCTCAGAGAACCTTCGAAAAACCGCCCTGCAAGGCGGTTT TTTCGTTTTCAGAGCAAGAGATTACGCGCAGACCAAAACGATCTCAAGAAGATCATCT TATTAAGGGGTCTGACGCTCAGTGGAACGAAAACTCACGTTAAGGGATTTTGGTCATG AGATTATCAAAAAGGATCTTCACCTAGATCCTTTTAAATTAAAAATGAAGTTTTAAAT CAATCTAAAGTATATATGAGTAAACTTGGTCTGACAGTTACCAATGCTTAATCAGTGA GGCACCTATCTCAGCGATCTGTCTATTTCGTTCATCCATAGTTGCCTGACTCCCCGTC GTGTAGATAACTACGATACGGGAGGGCTTACCATCTGGCCCCAGTGCTGCAATGATAC CGCGAGACCCACGCTCACCGGCTCCAGATTTATCAGCAATAAACCAGCCAGCCGGAAG GGCCGAGCGCAGAAGTGGTCCTGCAACTTTATCCGCCTCCATCCAGTCTATTCCATGG TGCCACCTGACGTCTAAGAAACCATTATTATCATGACATTAACCTATAAAAATAGGCG TATCACGAGGCAGAATTTCAGATAAAAAAAATCCTTAGCTTTCGCTAAGGATGATTTC TGGAATTCGCGGCCGCTTCTAGAG

Table S8: List of plasmid circuit constructs used in this study.

Plasmid	Description	Reference
pSB3K3	BioBrick vector, p15A ori, Kan^r	iGEM Registry[15]
pBW100ParsR	pSB3K3 carrying *J101-rbs32-arsR-t*-P_{arsR}	This study
pBW101ParsR-gfp	pSB3K3 carrying *J101-rbs32-arsR-t*-P_{arsR}-30*gfp*-t	This study
pBW102ParsR-Amp32^C	pBW100ParsR carrying 30*hrpR*-32*hrpS*-t-*hrpL*-30*gfp*-t	This study
pBW103ParsR-Amp30^C	pSB3K3 carrying *J109*-30*hrpR*-30*hrpS*-t-*hrpL*-30*gfp*-t	This study
pBW110pBAD	pSB3K3 carrying *araC*-P_{BAD}	This study
pBW111pBAD-gfp	pSB3K3 carrying *araC*-P_{BAD}-30*gfp*-t	This study
pBW112pBAD-hrpV	pSB3K3 carrying *araC*-P_{BAD}-30*hrpV*-t	This study
pBW201J109-gfp	pSB3K3 carrying *J109*-30*gfp*-t	This study
pBW202J114-gfp	pSB3K3 carrying *J114*-30*gfp*-t	This study
pBW203J116-gfp	pSB3K3 carrying *J116*-30*gfp*-t	This study
pBW204J115-gfp	pSB3K3 carrying *J115*-30*gfp*-t	This study
pBW205J105-gfp	pSB3K3 carrying *J105*-30*gfp*-t	This study
pBW206J106-gfp	pSB3K3 carrying *J106*-30*gfp*-t	This study
pBW211J109-Amp32^C	pSB3K3 carrying *J109*-30*hrpR*-32*hrpS*-t-*hrpL*-30*gfp*-t	This study
pBW212J114-Amp32^C	pSB3K3 carrying *J114*-30*hrpR*-32*hrpS*-t-*hrpL*-30*gfp*-t	This study
pBW213J116-Amp32^C	pSB3K3 carrying *J116*-30*hrpR*-32*hrpS*-t-*hrpL*-30*gfp*-t	This study
pBW214J115-Amp32^C	pSB3K3 carrying *J115*-30*hrpR*-32*hrpS*-t-*hrpL*-30*gfp*-t	This study
pBW215J105-Amp32^C	pSB3K3 carrying *J105*-30*hrpR*-32*hrpS*-t-*hrpL*-30*gfp*-t	This study
pBW216J106-Amp32^C	pSB3K3 carrying *J106*-30*hrpR*-32*hrpS*-t-*hrpL*-30*gfp*-t	This study
pBW300ParsR-Amp32^T	pSB3K3 carrying *araC*-P_{BAD}-30*hrpV*-t-*J101-32arsR-t*-P_{arsR}-30*hrpR*-32*hrpS*-t-*hrpL*-30*gfp*-t	This study
pBW301ParsR-Amp30^T	pSB3K3 carrying *araC*-P_{BAD}-30*hrpV*-t-*J101-32arsR-t*-P_{arsR}-30*hrpR*-32*hrpS*-t-*hrpL*-30*gfp*-t	This study
pBW311J109-Amp32^T	pSB3K3 carrying *araC*-P_{BAD}-30*hrpV*-t-*J109*-30*hrpR*-32*hrpS*-t-*hrpL*-30*gfp*-t	This study
pBW312J114-Amp32^T	pSB3K3 carrying *araC*-P_{BAD}-30*hrpV*-t-*J114*-30*hrpR*-32*hrpS*-t-*hrpL*-30*gfp*-t	This study
pBW313J116-Amp32^T	pSB3K3 carrying *araC*-P_{BAD}-30*hrpV*-t-*J116*-30*hrpR*-32*hrpS*-t-*hrpL*-30*gfp*-t	This study
pBW314J115-Amp32^T	pSB3K3 carrying *araC*-P_{BAD}-30*hrpV*-t-*J115*-30*hrpR*-32*hrpS*-t-*hrpL*-30*gfp*-t	This study
pBW315J105-Amp32^T	pSB3K3 carrying *araC*-P_{BAD}-30*hrpV*-t-*J105*-30*hrpR*-32*hrpS*-t-*hrpL*-30*gfp*-t	This study
pBW316J106-Amp32^T	pSB3K3 carrying *araC*-P_{BAD}-30*hrpV*-t-*J106*-30*hrpR*-32*hrpS*-t-*hrpL*-30*gfp*-t	This study

Promoter characterisation for input transfer functions

P_{arsR} input

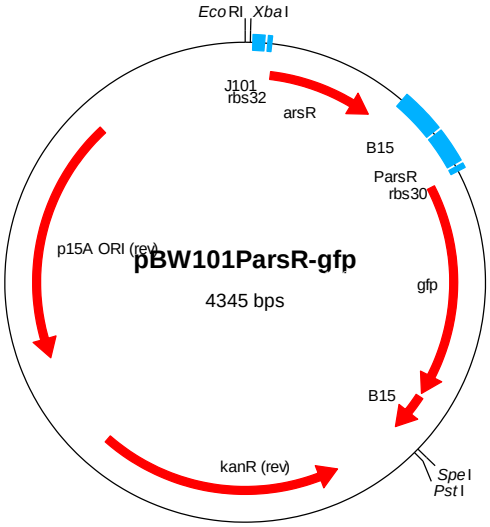

pSB3K3 carrying *J101-rbs32-arsR-t-*P_{arsR}*-*30*gfp*-t

Pc input (e.g J116)

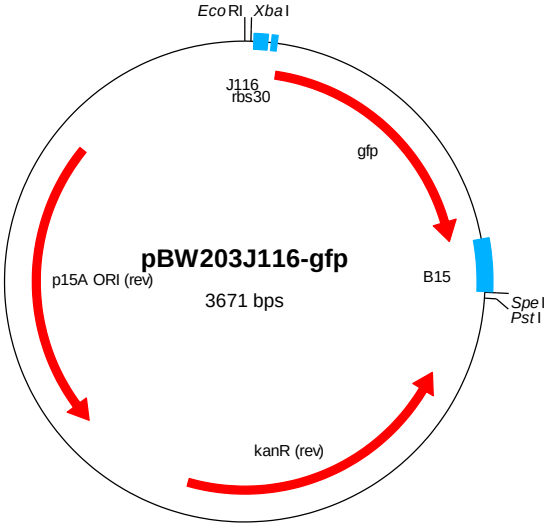

pSB3K3 carrying *J116*-30*gfp*-t

Gain-fixed amplifier using P_{arsR} (left) or P_C (right) as the input

P_{arsR} input

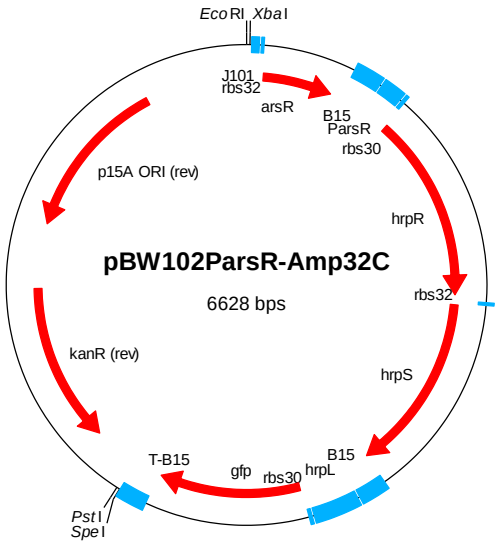

pBW100ParsR carrying 30*hrpR*-32*hrpS*-t-*hrpL*-30*gfp*-t

Pc input (e.g J116)

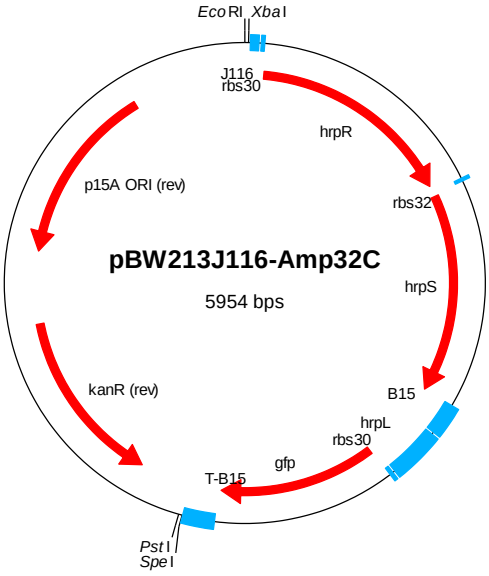

pSB3K3 carrying *J116*-30*hrpR*-32*hrpS*-t-*hrpL*-30*gfp*-t

Figure S16: Plasmids used for the gain-fixed amplifier characterisation with the arsenic sensor input or constitutive promoter input. The top two plasmids were used for the characterisation of the arsenic responsive sensor input (Fig. S1, Fig. 2B) and constitutive promoter input (Fig. S5A). The bottom two plasmids were used for the fixed-gain amplifier $Amp32^C$ characterisation (Fig. S2, Fig. 2A, Fig. 3D). To obtain $Amp30^C$, the rbs ahead of the *hrpS* gene was replaced by rbs30.

Gain-tunable amplifier using P_{arsR} or P_C as the input and P_{BAD} as the gain-tuning input

A

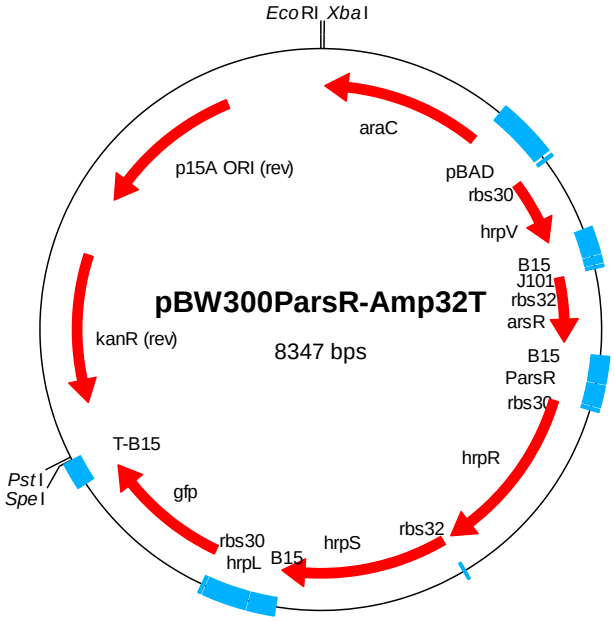

B

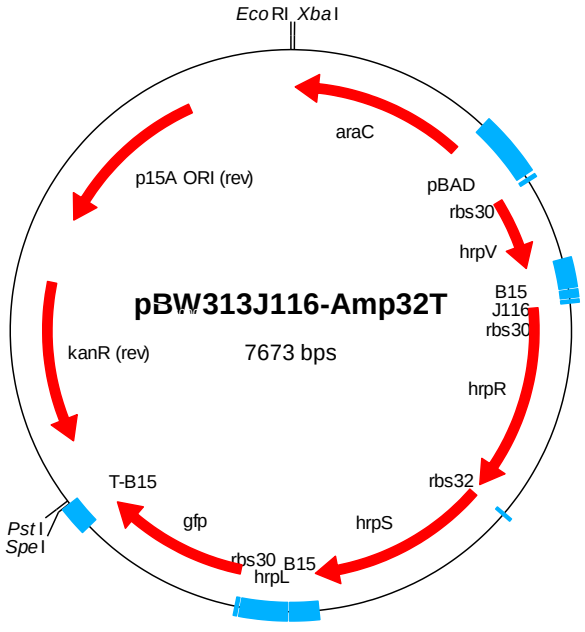

Figure S17: Plasmids used for the gain-tunable amplifier with the arsenic sensor input or constitutive promoter input. (**A**) The plasmid for encoding the gain-tunable amplifier $Amp32^T$ with arsenic sensor as the input (Fig. 4A-D). (**B**) The plasmid for encoding the gain-tunable amplifier $Amp32^T$ with constitutive promoters (e.g. J116) as the input (Fig. S9). To obtain $Amp30^T$, the rbs ahead of the *hrpS* gene was replaced by rbs30.

Supplementary References

1 Bushberg, J. T., Seibert, J. A., Leidholdt, E. M. & Boone, J. M. *The Essential Physics of Medical Imaging*. 2nd edn, (Lippincott Williams & Wilkins, 2006).
2 Coughlin, R. F. & Driscoll, F. F. *Operational Amplifiers and Linear Integrated Circuits*. 6th edn, (Prentice-Hall, 2000).
3 Yi, T.-M., Huang, Y., Simon, M. I. & Doyle, J. Robust perfect adaptation in bacterial chemotaxis through integral feedback control. *Proceedings of the National Academy of Sciences* 97, 4649-4653 (2000).
4 Alon, U. *An Introduction To Systems Biology: Design Principles Of Biological Circuits*. (Chapman & Hall/CRC, 2007).
5 Zoltan, S., Jörg, S. & Vipul, P. *System Modeling In Cell Biology: From Concepts To Nuts And Bolts*. (The MIT Press, 2006).
6 Wang, B., Kitney, R. I., Joly, N. & Buck, M. Engineering modular and orthogonal genetic logic gates for robust digital-like synthetic biology. *Nat. Commun.* 2, 508 (2011).
7 Jovanovic, M. *et al.* Regulation of the co-evolved HrpR and HrpS AAA+ proteins required for Pseudomonas syringae pathogenicity. *Nat. Commun.* 2, 177 (2011).
8 Preston, G., Deng, W.-L., Huang, H.-C. & Collmer, A. Negative Regulation of *hrp* Genes in *Pseudomonas syringae* by HrpV. *J. Bacteriol.* 180, 4532-4537 (1998).
9 Collmer, A. *et al. Pseudomonas syringae* Hrp type III secretion system and effector proteins. *Proc Natl Acad Sci USA* 97, 8770-8777 (2000).
10 Diorio, C., Cai, J., Marmor, J., Shinder, R. & DuBow, M. S. An *Escherichia coli* chromosomal ars operon homolog is functional in arsenic detoxification and is conserved in gram-negative bacteria. *J. Bacteriol.* 177, 2050-2056 (1995).
11 Guzman, L., Belin, D., Carson, M. & Beckwith, J. Tight regulation, modulation, and high-level expression by vectors containing the arabinose PBAD promoter. *J. Bacteriol.* 177, 4121-4130 (1995).
12 *Constitutive promoter family catalog*, <http://parts.igem.org/Promoters/Catalog/Anderson> (2013).
13 *B0015 double terminator*, <http://parts.igem.org/Part:BBa_B0015> (2013).
14 *Greem fluorescent protein derived from jellyfish Aequeora victoria* <http://parts.igem.org/Part:BBa_E0040> (2013).
15 *pSB3K3 plasmid backbone*, <http://parts.igem.org/Part:pSB3K3> (2013).
16 Shetty, R., Endy, D. & Knight, T. Engineering BioBrick vectors from BioBrick parts. *J. Biol. Eng.* 2, 5 (2008).